American Journal of Case Reports

e-ISSN 1941-5923
© Am J Case Rep, 2026; 27: e953317
DOI: 10.12659/AJCR.953317

Received: 2026.03.05
Accepted: 2026.07.22
Available online: 2026.08.31
Published: 2026.XX.XX

Contrast-Enhanced Ultrasound Combined With Biopsy for the Preoperative Diagnosis of a Rare Pelvic Schwannoma: a Case Report

Authors' Contribution:
Study Design A
Data Collection B
Statistical Analysis C
Data Interpretation D
Manuscript Preparation E
Literature Search F
Funds Collection G

ABEF Jinzhe Wang
AD Li Wei
BF Yufei Wang

Department of Ultrasound, Yichang Central People's Hospital, The First College of Clinical Medical Science, China Three Gorges University, Yichang, Hubei, PR China

Corresponding Author: Li Wei, No. 183, Yiling Avenue, Wujiagang District, Yichang City, Hubei Province, China
Phone: +13872454780, e-mail: wlultrasound@163.com

Financial support: None declared
Conflict of interest: None declared

Patient: Male, 66-year-old
Final Diagnosis: Benign pelvic schwannoma
Symptoms: Dysuria • lower abdominal pain • lumbago
Clinical Procedure: —
Specialty: Radiology

Objective: Rare disease

Background: Primary pelvic schwannomas are rare and often misdiagnosed due to non-specific imaging features. Accurate preoperative evaluation remains a challenge. The clinical utility of contrast-enhanced ultrasound (CEUS) combined with time-intensity curve (TIC) analysis and targeted biopsy was evaluated for the preoperative diagnosis and management of a pelvic schwannoma.

Case Report: A 66-year-old man presented with dysuria and lumbago. Imaging revealed a large, mixed cystic-solid pelvic mass. Conventional ultrasound demonstrated a predominantly cystic-solid lesion with limited Doppler flow, whereas CEUS showed progressive dendritic enhancement of the viable solid component from the periphery toward the center, with non-enhancement of cystic or necrotic areas. TIC analysis demonstrated a distinctive "equal-in and slow-out" perfusion pattern, supported by quantitative parameters (rise time, time to peak, fall time, and washout area under the curve). Based on these perfusion characteristics, ultrasound-guided biopsy was directed toward hyperenhanced viable regions while avoiding necrotic zones, thereby improving tissue sampling accuracy. Immunohistochemistry confirmed S-100 and SOX-10 positivity, establishing a definitive diagnosis. Complete surgical resection with bladder defect repair was performed. Postoperatively, urinary function recovered, and no recurrent urinary or pelvic symptoms were reported during outpatient follow-up.

Conclusions: Quantitative CEUS-TIC analysis combined with targeted biopsy provides an effective preoperative diagnostic strategy for pelvic schwannomas. The observed CEUS-TIC perfusion pattern may correspond to the heterogeneous microvascular distribution of Antoni A and Antoni B regions; however, this hypothesis requires validation in future imaging-pathology correlation studies.

Keywords: Magnetic Resonance Angiography • Neurilemmoma • Ultrasonography, Interventional

Full-text PDF: https://www.amjcaserep.com/abstract/index/idArt/953317

Indexed in: [PMC] [PubMed] [Emerging Sources Citation Index (ESCI)] [Web of Science by Clarivate]

Introduction

Primary pelvic schwannomas are rare soft tissue neurogenic tumors arising from the sacral nerves or inferior hypogastric plexus, accounting for less than 1% of all schwannomas [1]. Most lesions are benign and encapsulated [2]. Due to the deep anatomical location and expansive pelvic cavity, pelvic schwannomas often grow insidiously and remain asymptomatic in early stages [3]. Symptoms generally appear only when the mass significantly enlarges and compresses adjacent nerves or organs. Pelvic schwannomas can be easily misdiagnosed as genitourinary or intestinal tumors due to nonspecific symptoms [4]. Large tumors may adhere to adjacent tissues such as the bladder and ureter, complicating surgical resection and increasing the risk of complications, including nerve injury, which can affect prognosis [5].

Conventional modalities, including computed tomography (CT) and magnetic resonance imaging (MRI), provide valuable anatomical detail but often lack specificity in differentiating pelvic schwannomas from other masses. Quantitative contrast-enhanced ultrasound (CEUS) with time-intensity curve (TIC) analysis offers functional evaluation of tissue perfusion, yet its application in pelvic schwannomas remains virtually unexplored [6]. This report describes a case of pelvic schwannoma evaluated preoperatively using CEUS with TIC quantitative analysis. The correlation between CEUS features and histopathology was analyzed. Based on these perfusion characteristics, targeted sampling of viable tissue via ultrasound-guided biopsy was conducted, while avoiding necrotic regions. Immunohistochemistry confirmed S-100 and SOX-10 positivity, establishing a definitive diagnosis [7]. Complete surgical resection of the tumor is the preferred treatment for pelvic schwannoma [1]. The specific CEUS-TIC perfusion pattern observed in this case may reflect the heterogeneous microvascular architecture of Antoni A and Antoni B regions, representing a potential imaging-pathology correlation that has been rarely reported. This case illustrates the utility of CEUS-TIC as a noninvasive diagnostic tool, which may reduce preoperative misdiagnosis and guide surgical planning for rare pelvic schwannomas.

Case Report

The patient was a 66-year-old Han Chinese man who presented with urinary difficulty and lower back and abdominal pain for 1 week. He had no nausea or vomiting, chills, fever, or other associated symptoms. His medical history included hypertension (4 years, on nifedipine 30 mg once daily), gout (> 20 years, on intermittent allopurinol), and right sciatica (> 10 years, on intermittent ibuprofen). He had no history of smoking, alcohol, substance abuse, or hereditary diseases in the family.

On physical examination, slight abdominal distension was noted in the lower abdomen, with a palpable mass approximately 120 × 110 mm in the pelvic region. The mass was soft, moderately mobile, tender on palpation, and without rebound tenderness. Bilateral renal percussion tenderness was positive. After admission, the patient underwent comprehensive laboratory tests. Laboratory tests revealed leukocytosis (white blood cells 11.0×10^9 cells/L), neutrophilia (78%), elevated C-reactive protein (CRP; 25 mg/L), and microscopic urine analysis showed elevated non-squamous epithelial cells (3.7 cells/μl), indicating a urinary tract infection. The patient received intravenous levofloxacin 0.5 g once daily for 5 days, which resolved the infection.

Imaging Evaluation

Conventional ultrasound revealed a well-circumscribed mixed cystic-solid pelvic mass measuring 129 × 96 × 120 mm, with

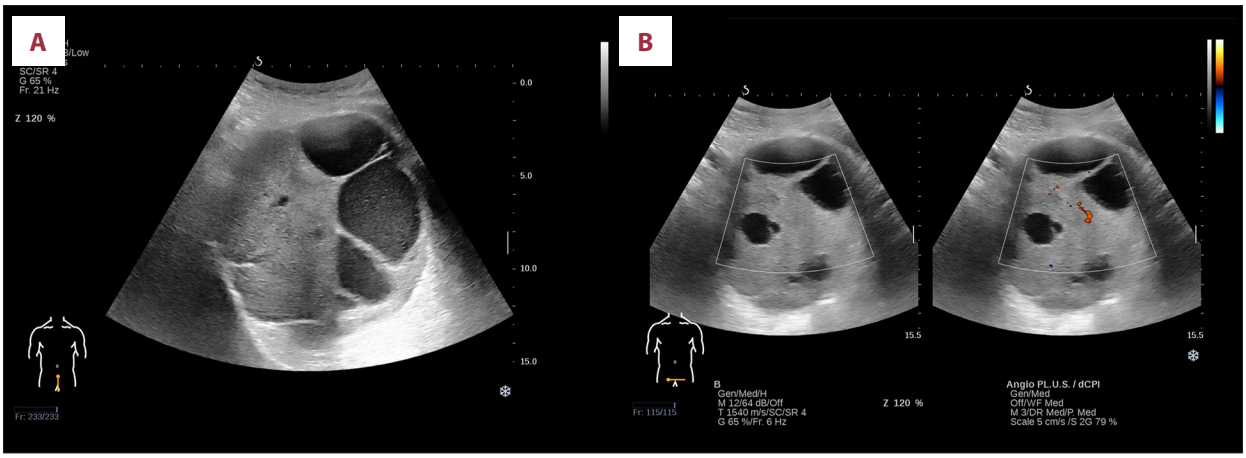

Figure 1. Conventional ultrasound of pelvic schwannoma. (**A**) Longitudinal view showing a well-circumscribed, mixed cystic-solid hypoechoic mass with multiple anechoic areas. (**B**) Transverse color Doppler image demonstrating minimal internal blood flow.

Indexed in: [PMC] [PubMed] [Emerging Sources Citation Index (ESCI)] [Web of Science by Clarivate]

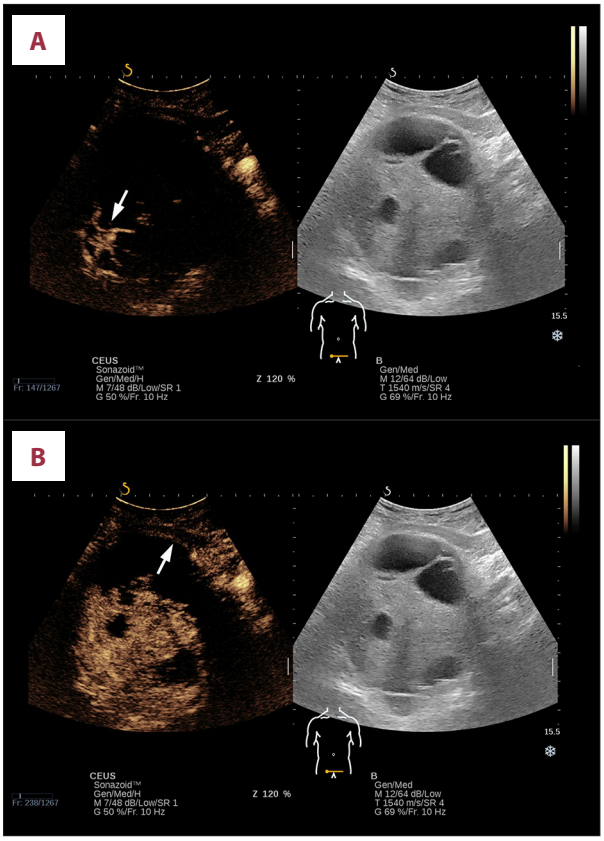

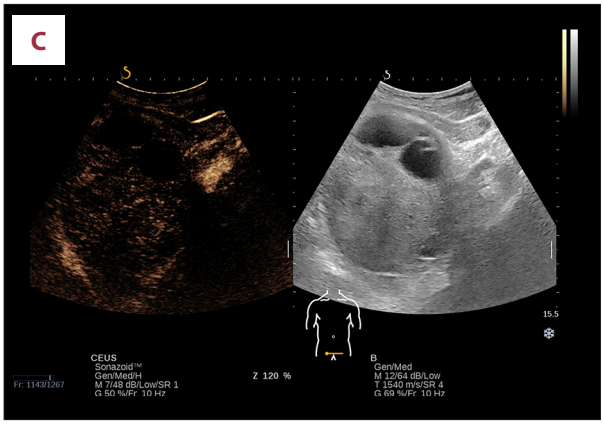

Figure 2. Contrast-enhanced ultrasound of pelvic schwannoma. (**A**) Early phase (11 s) showing tree-like enhancement of the solid component and capsule from periphery to center (arrows). (**B**) Mid-phase (24 s) showing progressive enhancement of the solid component with scattered non-enhancing areas; capsule remains intact (arrows); cystic component remains non-enhancing. (**C**) Late phase (38 s) showing delayed washout of the solid component with uneven low enhancement.

moderate echogenicity in the solid portion and poor acoustic transmission in the cystic portion. Minimal blood flow signals were detected in the solid component (**Figure 1**). For this giant cystic-solid pelvic mass, differential diagnoses were considered to include a neurogenic tumor, particularly schwannoma, as well as a gastrointestinal stromal tumor, a genitourinary tract neoplasm, and a retroperitoneal sarcoma. However, given the cystic-solid morphology, sparse intralesional vascularity, and intact capsule, the lesion was considered more likely to represent a benign or low-grade malignant tumor. CEUS images visually demonstrated dendritic enhancement progressing from the periphery toward the center of the tumor (**Figure 2**). Quantitative TIC analysis confirmed an overall "equal-in, slow-out" perfusion pattern within the solid component (**Figure 3**). In particular, the peripheral-to-central dendritic enhancement pattern and the "equal-in and slow-out" enhancement characteristics demonstrated on CEUS were considered more suggestive of a benign tumor. Contrast-enhanced MRI further delineated a cystic-solid mass (127 × 95 × 113 mm) with isointense solid component on T1, high-signal cystic component on T2 fat-suppressed sequences, and heterogeneous solid enhancement displacing the bladder and surrounding tissues (**Figure 4**). On contrast-enhanced MRI, a benign tumor was further favored by the well-circumscribed morphology, heterogeneous enhancement, cystic degeneration, and displacement rather than definite invasion of adjacent pelvic structures, with a neurogenic origin considered more likely. Integration of multimodal imaging suggested a benign neurogenic tumor, likely a schwannoma.

Histopathological Confirmation

Ultrasound-guided needle biopsy targeting viable tissue and avoiding necrotic areas was conducted. Pathology revealed spindle cell lesions with benign morphology, lipid-rich histiocytes, and no mitotic figures. Immunohistochemistry results were as follows: S-100 (+), SOX-10 (+), Ki-67 (~2%); SMA (-), CD117 (-), CD34 (-), Desmin (-), DOG-1 (-), PCK (-), supporting schwannoma diagnosis.

After resolving the patient's urinary tract infection, pelvic adhesiolysis and complete tumor excision were performed. Intraoperatively, the tumor was tightly adherent to the ureterovesical junction, so bilateral ureteral stents were placed to prevent ureteral injury and stricture. The resected specimen was a grayish-red nodular mass (150 × 120 × 70 mm) with an intact capsule, a cystic-solid appearance on sectioning, and soft consistency (**Figure 5A**). Postoperative immunohistochemistry confirmed schwannoma, consistent with the preoperative biopsy findings (**Figure 5B, 5C**). The patient recovered well postoperatively. On postoperative day 4, CT showed unobstructed drainage and no hydronephrosis. By day 8, the pelvic drainage tube was removed, and the urinary catheter remained in situ. At the 2-week outpatient follow-up, the patient's pain had subsided and the catheter was removed. Six-week follow-up confirmed successful removal of bilateral ureteral stents, with unobstructed urination and no urinary symptoms. Regular follow-up was advised.

Indexed in: [PMC] [PubMed] [Emerging Sources Citation Index (ESCI)] [Web of Science by Clarivate]

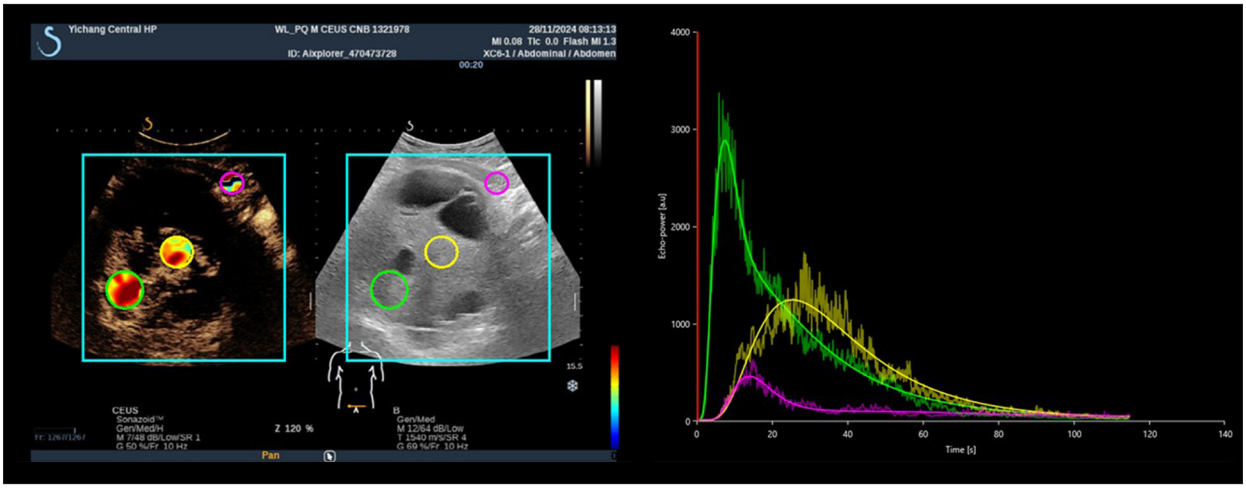

Figure 3. CEUSTIC analysis of pelvic schwannoma. ROI1: peripheral tumor region (green); ROI2: central tumor region (yellow); ROI3: adjacent normal tissue (pink). The time to initial enhancement for ROI1/ROI2 was 10.68 s and 12.55 s, respectively, with a difference of no more than 2.3 s compared with ROI3 (12.86 s), demonstrating an "equal-in" pattern. Late-phase enhancement showed WoAUC [au] values of 2.42×10^4 and 2.96×10^4 for ROI1/ROI2, versus 4.10×10^3 for ROI3, consistent with a "slow-out" pattern. ROI1 reached its peak earlier (TTP: 7.48 s vs 25.41 s) and exhibited higher peak intensity (PE: 2.87×10^3 au vs 1.23×10^3 au). CEUS, contrast-enhanced ultrasound; TIC, time-intensity curve; ROI, region of interest; WoAUC, washout area under the curve; TTP, time to peak.

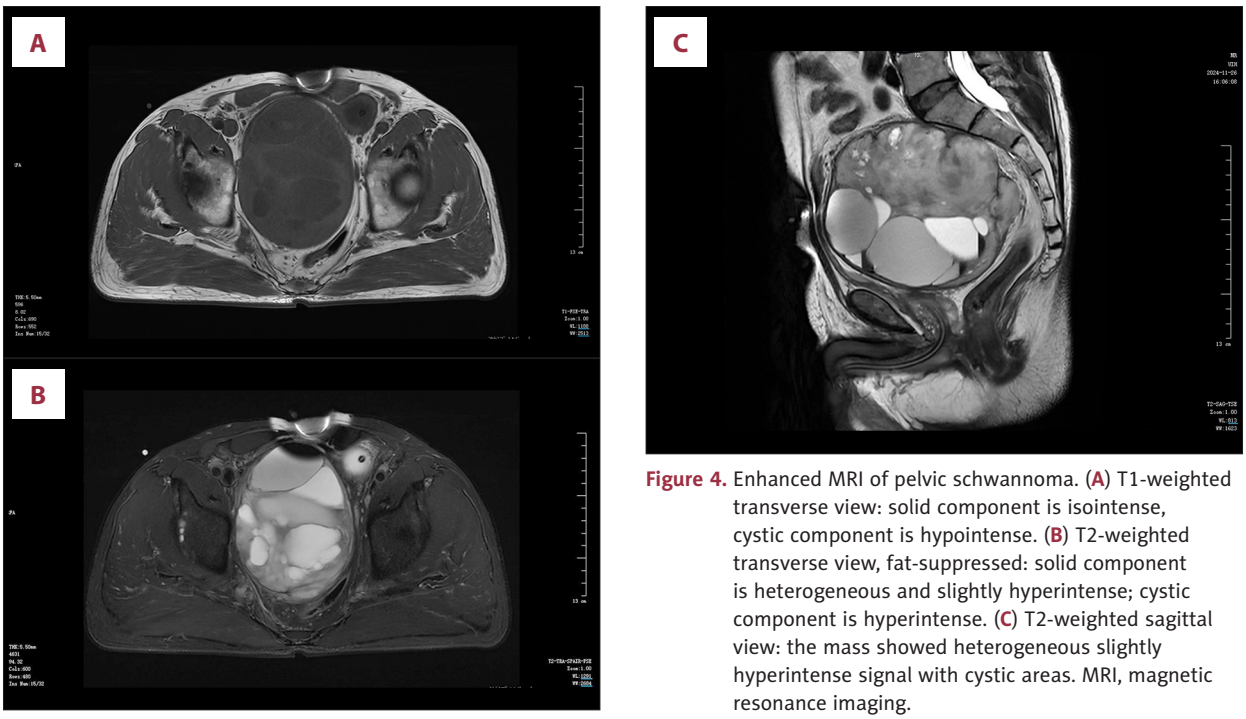

Figure 4. Enhanced MRI of pelvic schwannoma. (**A**) T1-weighted transverse view: solid component is isointense, cystic component is hypointense. (**B**) T2-weighted transverse view, fat-suppressed: solid component is heterogeneous and slightly hyperintense; cystic component is hyperintense. (**C**) T2-weighted sagittal view: the mass showed heterogeneous slightly hyperintense signal with cystic areas. MRI, magnetic resonance imaging.

Discussion

Pelvic schwannoma is a rare benign tumor originating from Schwann cells, accounting for less than 1% of all schwannomas. Due to its deep location and lack of early symptoms, it is often misdiagnosed as a tumor of the urinary or reproductive system [8]. In this case, the patient presented with dysuria and lumbar-abdominal pain, and imaging revealed a large cystic-solid pelvic mass. Regarding imaging evaluation, contrast-enhanced MRI is considered the gold standard for schwannoma characterization due to its superior soft tissue resolution [9]. Typical manifestations include isointense or hypointense signals on T1-weighted images, heterogeneous hyperintense signals on T2-weighted images with cystic areas, and heterogeneous

Indexed in: [PMC] [PubMed] [Emerging Sources Citation Index (ESCI)] [Web of Science by Clarivate]

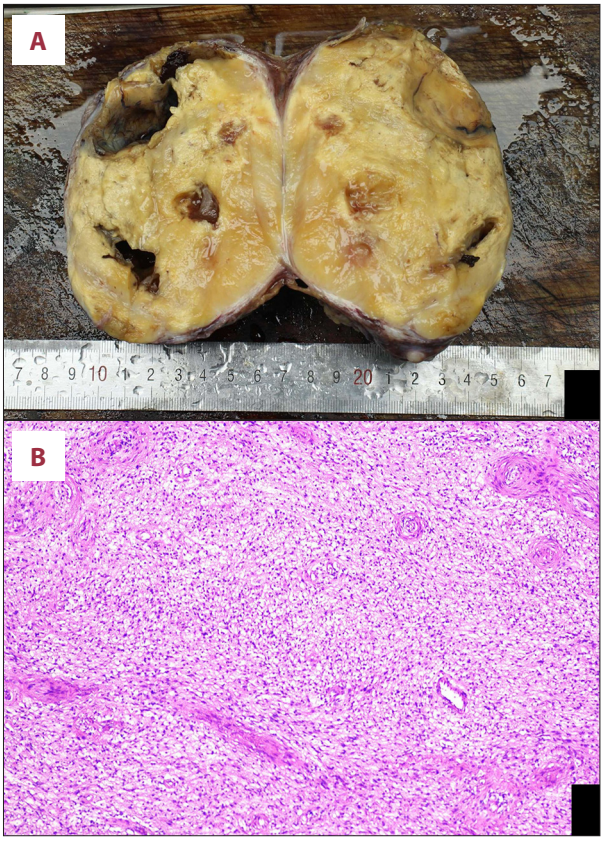

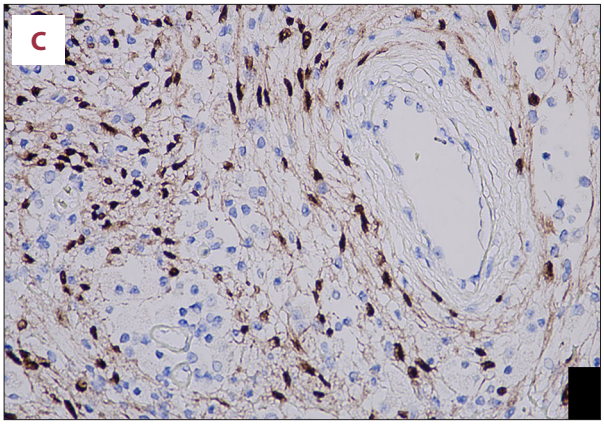

Figure 5. Histopathology and immunohistochemistry of the pelvic schwannoma. (**A**) Gross specimen showing a tumor with cystic spaces of varying sizes. (**B**) Hematoxylin and eosin (H&E) staining showing spindle-shaped cells with benign morphology and interspersed lipid-rich histiocytes. No mitotic figures were observed (H&E × 10). (**C**) Immunohistochemistry showing SOX-10 positivity.

enhancement after contrast administration [10,11]. The MRI findings in this case are highly consistent with the aforementioned characteristics. However, due to its affordability and convenience, ultrasound is the preferred screening method for pelvic masses. In this case, conventional ultrasound clearly revealed the cystic-solid structure, capsule integrity, and internal vascular distribution. CEUS with TIC analysis provided additional functional information, revealing a characteristic "equal-in, slow-out" perfusion pattern suggestive of a benign lesion [12]. These findings supported proceeding with complete surgical excision.

In this case, CEUS demonstrated a progressive dendritic enhancement extending from the periphery toward the center, which may reflect the intratumoral distribution of microvasculature. Schwannomas are typically composed of compact Antoni A and loosely arranged Antoni B regions, each with distinct pathological features. Antoni A regions, being cell-rich and metabolically active, possess relatively higher microvascular density, allowing the contrast agent to enter more rapidly and concentrically, resulting in early enhancement. In contrast, Antoni B regions, rich in myxoid stroma, generally exhibit weaker enhancement [13]. The dendritic areas observed on CEUS likely correspond predominantly to Antoni A regions. Detailed TIC analysis revealed that the peripheral region of interest (ROI1) had a time to peak (TTP) of 7.48 s, whereas the central region (ROI2) had a TTP of 25.41 s, confirming the differential perfusion kinetics across tumor regions. Regarding enhancement intensity, the peak enhancement of ROI1 was significantly higher than ROI2, reflecting more abundant peripheral blood supply and higher cellular activity.

Most previous studies have described a central-to-peripheral "target sign" [14], whereas this case provides the first evidence of a peripheral-to-central dendritic enhancement pattern. These findings are presented with the caveat that they are based on a single-case observation and do not yet elucidate the mechanistic basis of the enhancement pattern or its diagnostic value in schwannomas. Further studies with larger cohorts are needed to validate these observations. Furthermore, in this case, the delayed washout observed in ROI2 contrasts with the typically faster washout reported for Antoni B regions. This discrepancy may be explained by the following mechanisms: Antoni B regions, characterized by sparse, dilated vessels within a myxoid stroma, inherently exhibit slower perfusion. In a markedly enlarged tumor, chronically elevated interstitial pressure further compresses and distorts these vessels, creating microvascular stasis — a "retention pool" — that slows microbubble clearance, producing the observed "slowout" pattern. Conversely, the Antoni A region at the tumor periphery maintains structurally intact vasculature under lower interstitial pressure, preserving rapid perfusion and washout. These observations suggest that CEUS washout kinetics in large pelvic schwannomas are influenced not only by histological subtype but also by tumor size, local interstitial pressure gradients, and associated hemodynamic changes. The relative impact of intrinsic tissue architecture versus extrinsic compressive forces remains to be systematically investigated in future hemodynamic-pathological correlation studies.

Indexed in: [PMC] [PubMed] [Emerging Sources Citation Index (ESCI)] [Web of Science by Clarivate]

Ultrasound-guided needle biopsy was then conducted, targeting the perfused regions identified by CEUS and avoiding cystic or necrotic areas and ensuring high-quality tissue sampling. Histopathology and immunohistochemistry confirmed S-100 and SOX-10 positivity, with a low Ki-67 index (~2%), providing decisive evidence for schwannoma. SOX-10, as a neural crest transcription factor, is highly specific for Schwann cell-derived tumors, and combined with S-100, it enhances diagnostic accuracy [6,15].

Regarding treatment, complete surgical excision remains the standard approach for pelvic schwannomas due to their anatomical location and benign nature [16]. In this case, the tumor was solitary, encapsulated, and well-defined, allowing for simple excision. In more complex cases, care is required to prevent nerve injury, as an incomplete microsurgical technique may result in permanent dysfunction and pain [5]. The patient in this report did not undergo combined microsurgical intervention, which represents a potential limitation of the treatment strategy. Furthermore, due to the large size of the tumor (maximum diameter > 10 cm) and its extensive adhesions to surrounding tissues, conventional MRI sequences could not clearly trace the continuity between the tumor and specific sacral nerve roots. Moreover, this patient did not undergo dedicated magnetic resonance neurography (MRN) sequences, such as 3-dimensional short T1 inversion recovery (STIR), sampling perfection with application-optimized contrast using different flip angle evolution (SPACE) or diffusion-weighted whole-body imaging with background body signal suppression (DWIBS), precluding precise preoperative localization of the originating nerve roots (eg, S1, S2, or S3). Based on anatomical landmarks, the tumor center was estimated to be at the S2-to-S3 level, potentially arising from the sacral plexus or inferior hypogastric plexus at this level. Therefore, we recommend that future studies employ high-resolution MRN combined with intraoperative electrophysiological monitoring to achieve more accurate nerve root localization [17].

Conclusions

Pelvic schwannomas are rare, and both clinical presentation and conventional imaging lack specificity. In this case, CEUS-TIC analysis revealed a characteristic dendritic perfusion pattern in the solid tumor component, which is hypothesized to correspond to the heterogeneous microvascular distribution of Antoni A and Antoni B regions. Ultrasound-guided targeted biopsy enabled accurate pathological diagnosis, confirming schwannoma and guiding optimal preoperative surgical planning. Multimodal imaging, including CEUS and MRI, provided complementary diagnostic information. This report supplements current knowledge on the imaging features of pelvic schwannomas, potentially enhancing clinicians' awareness and reducing misdiagnosis. Future studies with larger cohorts are needed to validate this observation and explore the utility of CEUS-TIC in preoperative planning.

Institution Where Work Was Done

Yichang Central People's Hospital, Yichang, Hubei, PR China.

Declaration About Informed Consent

Written informed consent was obtained from the patient for the publication of this case report and any accompanying de-identified clinical information and images.

Declaration of Figures' Authenticity

All figures submitted have been created by the authors who confirm that the images are original with no duplication and have not been previously published in whole or in part.

References:

1. Smyth SL, Dhar S, Cogswell ML, Majd HS. Ten-step surgical approach to management of pathology of the ischiorectal fossa-a review of the literature and application in a rare pelvic schwannoma. J Invest Surg. 2021;35(5):1067-73
2. Andrej O, Lucija V, Mirko O. Giant pelvic schwannoma presenting with increased urinary frequency – Case report. Int J Surg Case Rep. 2022;93:106934
3. Maidarti M, Wibawa YS, Garinasih PD, et al. Rare case of pelvic schwannoma mimicking intra-ligamenter uterine fibroid: A case report. Int J Surg Case Rep. 2022;96:107327
4. Fischerova D, Santos G, Wong L, et al. Imaging in gynecological disease (26): Clinical and ultrasound characteristics of benign retroperitoneal pelvic peripheral-nerve-sheath tumors. Ultrasound Obstet Gynecol. 2023;62(5):727-38
5. Benato A, D'Alessandris QG, Murazio M, et al. Integrated neurosurgical management of retroperitoneal benign nerve sheath tumors. Cancers (Basel). 2023;15(12):3138
6. Fan S, Wang H, Sun X, et al. Comprehensive analysis of diagnosis and treatment in 99 cases of abdominal schwannoma. Cancer Med. 2024;13(16):e70140
7. Zohra BF, Amine N, Hajar Z, et al. Retroperitoneal pelvic schwannoma: A rare case report and review of the literature. Radiol Case Rep. 2024;19(8):3028-32
8. Tang Q, Liu XH, Hu ZD, Shao J. Analysis of ultrasonic features of pelvic retroperitoneal schwannomas. Chinese J Ultrasound Med. 2026;42(02):255-58
9. Santos AJ, Duarte L, Santos SC, Casimiro C. A 68-year-old woman presenting with recurrent abdominal pain and a diagnosis of a presacral retroperitoneal benign schwannoma that mimicked an ovarian tumor on pelvic magnetic resonance imagining. Am J Case Rep. 2022;23:e935985
10. Zeng SX, Wang L, Li Y. CT and MRI diagnosis of pelvic giant schwannoma: A case report. Chinese J CT MRI. 2024;22(01):185-86
11. Wu X, Meng H, Fan Q, et al. Image features and clinical analysis of retroperitoneal pelvic schwannoma: A case report. BMC Neurol. 2024;24(1):230
12. Evans DG, Mostaccioli S, Pang D, et al. ERN GENTURIS clinical practice guidelines for the diagnosis, treatment, management and surveillance of people with schwannomatosis. Eur J Hum Genet. 2022;30(7):812-17

Indexed in: [PMC] [PubMed] [Emerging Sources Citation Index (ESCI)] [Web of Science by Clarivate]

13. Lee MW, Joo DC, Kim GH, et al. Contrast-enhanced harmonic endoscopic ultrasonography for diagnosing gastric subepithelial tumors. Diagnostics (Basel). 2026;16(1):165
14. Helbing DROL, Schulz A, Morrison H. Pathomechanisms in schwannoma development and progression. Oncogene. 2020;39(32):5421-29
15. Yang L, Cui LG. "Target sign" of schwannoma on contrast-enhanced ultrasound. J Ultrasound Med. 2025;44(10):1927-35
16. Sanchez SI, Cimino-Mathews A. Breast schwannoma: Review of entity and differential diagnosis. J Pathol Transl Med. 2025;59(6):353-60
17. Xiao HT, Xu CX, Liu RY, et al. Clinical analysis of patients with primary pelvic retroperitoneal tumor. Chinese J Clin Oncol. 2023;50(15):786-90
18. Bulisani BM, Ströher M, Rossi FMB, et al. Robotic-assisted resection of a benign schwannoma of the obturator nerve: A rare case. Am J Case Rep. 2024;25:e942083
19. Eajazi A, Udayakumar D, Daftaribesheli L, et al. Whole-body magnetic resonance neurography-technique, current perspectives, and future directions. Magn Reson Imaging Clin N Am. 2025;33(3):411-26

Indexed in: [PMC] [PubMed] [Emerging Sources Citation Index (ESCI)] [Web of Science by Clarivate]